

PAPER • OPEN ACCESS

X-ray diffraction and infrared spectroscopy analyses on the crystallinity of engineered biological hydroxyapatite for medical application

To cite this article: G M Poralan Jr *et al* 2015 *IOP Conf. Ser.: Mater. Sci. Eng.* **79** 012028

View the [article online](#) for updates and enhancements.

You may also like

- [Effect of Combination of Anionic Polymer with Calcium Phosphate Coating on Corrosion Behavior of Magnesium Alloy in Physiological Solution](#)
Sachiko Hiromoto and Kotaro Doi
- [Fabrication and Characterisation of Gelatine/Hydroxyapatite Porous Scaffold](#)
M.I. Mazlam, H.H. Ho and A. Nurazreena
- [Implant application of bioactive nano-hydroxyapatite powders—a comparative study](#)
Karthik Alagarsamy, Vinita Vishwakarma, Gobi Saravanan Kaliaraj *et al.*



ECS
The
Electrochemical
Society
Advancing solid state &
electrochemical science & technology

DISCOVER
how sustainability
intersects with
electrochemistry & solid
state science research

X-ray diffraction and infrared spectroscopy analyses on the crystallinity of engineered biological hydroxyapatite for medical application

G M Poralan Jr^{1,3}, J E Gambe¹, E M Alcantara² and R M Vequizo¹

¹Materials Science, Laboratory, Physics Department, MSU - Iligan Institute of Technology, A. Bonifacio Avenue, Tibanga, 9200 Iligan City, Philippines

²College of Arts and Sciences, Capitol University, Corrales Avenue Osmeña St., 9000 Cagayan de Oro City, Philippines

Email: gilbertporalan@gmail.com, vequizorey2@gmail.com, diyes2003@gmail.com, eric_gordon19@yahoo.com

Abstract. Biological hydroxyapatite (BHAp) derived from thermally-treated fish bones was successfully produced. However, the obtained biological HAp was amorphous and thus making it unfavorable for medical application. Consequently, this research exploits and engineers the crystallinity of BHAp powders by addition of CaCO₃ and investigates its degree of crystallinity using XRD and IR spectroscopy. On XRD, the HAp powders with [Ca]/[P] ratios 1.42, 1.46, 1.61 and 1.93 have degree of crystallinity equal to 58.08, 72.13, 85.79, 75.85% and crystal size equal to 0.67, 0.74, 0.75, 0.72 nm, respectively. The degree of crystallinity and crystal size of the obtained calcium deficient biological HAp powders increase as their [Ca]/[P] ratio approaches the stoichiometric ratio by addition of CaCO₃ as source of Ca²⁺ ions. These results show the possibility of engineering the crystallinity and crystal size of biological HAp by addition of CaCO₃. Moreover, the splitting factor of PO₄ vibration matches the result with % crystallinity on XRD. Also, the area of phosphate-substitution site of PO₄ vibration shows linear relationship ($R^2=0.994$) with crystal size calculated from XRD. It is worth noting that the crystallinity of the biological HAp with [Ca]/[P] ratios 1.42 and 1.48 fall near the range 60-70% for highly resorbable HAp used in the medical application.

1. Introduction

Hydroxyapatite (HAp) with the chemical formula Ca₁₀(PO₄)₆(OH)₂ is one of the most important bioceramic material that has been extensively used in orthopedics and dentistry for implant fabrication and drug delivery system owing to its biocompatibility and bioactivity [1]. Numerous types of natural or synthetic HAp are commercially available not only for use in the biomedical field but also for chromatographic and catalytic applications [2]. In addition, it has been an excellent material for ion exchange material [2], adsorbent [2], ionic conductor [2], chemical gas sensor [3], fuel cells [4], physical sunscreen and sunscreen firming [5].

Hydroxyapatite derived from thermally-treated fish bones was successfully produced. However, the obtained biological HAp is calcium deficient and amorphous. In medical application, amorphous HAp

³ To whom any correspondence should be addressed.

is unfavorable when used for bone graft because of its very fast dissolution rate. Recent studies found out that the resorbability of HAp can be developed by controlling its degree of crystallinity to 60–70% and reducing its grain size to nanolevel [6,7]. This study aims to investigate the HAp powders with crystallinity useful in the medical application by engineering the produced amorphous HAp from thermally-treated fish bones by addition of CaCO_3 . X-ray diffraction (XRD) is used to characterize the phase composition and degree of crystallinity of the produced biological HAp. Additionally, infrared spectroscopy is used to elucidate the degree of crystallinity of HAp by establishing an index of crystallinity.

Considering the crystallography of HAp, it occurs as a hexagonally packed crystal belonging to $\text{P6}_3/\text{m}$ space group. The unit cell consists of Ca^{2+} , PO_4^{2-} , and OH^- groups closely packed together in a hexagonal arrangement. The OH^- group serves as the backbone for HAp. The six phosphates, PO_4 , are in a helical arrangement around the c -axis. These phosphate groups form a skeletal frame structural network which provides the stability of HAp. On X-ray diffraction, the crystallite size can be described by the diffracting plane (002) of HAp at $2\theta=25.50^\circ$ for the reason that this miller index correspond to the c -axis length. The full width at half maximum (FWHM) of the 002 reflection is inversely proportional to the crystallite length along the c unit cell direction (c -axis length) [8]. Thus, as HAp becomes more crystalline, the c -axis length increases which can be verified by the diffraction peak for (002) becoming narrower. Furthermore, the 100% crystalline HAp has diffraction peaks for (112) and (300) at equal intensities. Thus, the change in the ratio of the intensity of the trough between the (112) and (300) peaks to the intensity of (300) diffraction peak of HAp is a strong indication of change in the degree of crystallinity.

On infrared spectroscopy, information about the molecular components and structures are presented as a spectrum of absorption bands. At $500\text{--}620\text{ cm}^{-1}$ spectral region, the bending mode of PO_4 vibration consists of two peaks corresponding to transverse and longitudinal optical frequency. However, amorphous calcium phosphate gives a broad single absorption band in this region because of structural distortion on the lattice. As HAp becomes more crystalline, the hexagonal structure becomes evident. Consequently, the PO_4 vibration at this region becomes well define and a doublet peak is observed. Thus, this splitting of the bending mode of PO_4 vibration on the transformation of HAp from amorphous to crystalline phase can be an index of crystallinity. Furthermore, at $900\text{--}1200\text{ cm}^{-1}$ spectral region, a broadening of the spectra is observed between the anti-symmetric stretch modes of PO_4 vibration at 1040 and 1090 cm^{-1} . Incorporation of different types of anions in the HAp unit cell which affects the vibration of PO_4 and induces local structural distortions around these ions might be the reason of the broadening on this region [9]. Thus, the area of phosphate-substitution site might give as information on the crystal structure of HAp. These relationships between the planes (002), (112) and (300) for HAp as observed in XRD and the phosphate absorption bands of HAp on FTIR could be the bases on the correlation of the degree of crystallinity of HAp from the two characterization techniques.

This study opens a door for the modification of HAp by addition of CaCO_3 to tailor HAp phase which is good for biomedical applications. Additionally, the study on the crystallinity of this obtained HAp powders would greatly help in the production of quality HAp powders since crystallinity primarily influences the properties and performance of HAp.

2. Methodology

2.1. HAp powder preparation

The bones are boiled and washed then crushed and blended. Four samples are prepared and added with 0.2, 0.3, 0.4 and 0.5g CaCO_3 . The samples are then dissolved in a HNO_3 solution. The solution is heated at 150°C until only the powders are left. The dried samples are contained in a crucible then calcined for 5 hrs. at 900°C . The samples are subjected to FTIR spectroscopy for chemical purity, XRD for crystallographic properties and SEM-EDX for elemental composition. The crystallinity of the powder samples is elucidated from the obtained XRD and FTIR spectra.

2.2. Crystallinity and crystal size calculation using XRD characterization

The degree of crystallinity was calculated using diffraction peaks (112) and (300) of HAp with the equation [10] given as:

$$X_c = \frac{I_{300} - V_{112/300}}{I_{300}} \cdot 100 \quad [\%] \quad (1)$$

Where X_c is the fraction of crystalline phase, I_{300} is the intensity of (300) diffraction peak and $V_{112/300}$ is the intensity of the trough between (112) and (300) diffraction peaks of HAp. The range of 2θ where the peaks of interest fall is graphed separately. These peaks are then fitted using Gaussian/Lorentzian function in Qtiplot.

The average particle size is calculated from XRD data using the Debye–Scherrer approximation:

$$\tau = \frac{k\lambda}{\beta_{\tau} \cos \theta} \quad (2)$$

where τ is the particle size in nanometer, as calculated for the hkl reflection, k is the wavelength of $\text{Cu}_{K\alpha 1}$ radiation (1.5406 Å), β_{τ} is the full width at half maximum for the diffraction peak under consideration (in radian), θ is the diffraction angle and k is the broadening constant chosen as 0.9.

2.3. Index of crystallinity using FTIR spectroscopy

The splitting factor is taken as the area between peaks 570 and 602 cm^{-1} . The area is integrated using trapezoidal rule in Qtiplot. Afterwards, the selected region is fitted using Gaussian/Lorentzian function to obtain the FWHM of 602 cm^{-1} vibration.

2.4. Correlation of area of phosphate-substitution site and crystal size

The 900–1200 cm^{-1} spectral region is graphed using Qtiplot software. Lorentzian/Gaussian function is used for curve-fitting. For each spectrum, the regression coefficient is always better than 0.998 in order to have a consistent result. Initial peak positions are obtained from second-derivative spectra of the raw data. The area of the subband at approximately 1060 cm^{-1} is determined from the area given by the software from the fitting result. The calculated area of the subband is reported as a percentage of the total area of all the components. This method was presented by Pleshko *et al.* [8]. This area is labelled as %B and is graphed with respect to the crystal size calculated from XRD.

2.5. Characterizations

2.5.1. XRD characterization

X-ray diffraction (XRD) patterns are obtained in the range of $2\theta = 10\text{--}70^\circ$ using a step size of $0.02^\circ/\text{min}$ with a Shimadzu XRD-700 x-ray diffractometer operating at 40kV and 30mA producing $\text{Cu}_{K\alpha}$ with $\lambda = 0.154 \text{ nm}$. The obtained raw data are plotted using Qtiplot[®] free software for analysis of the samples followed by indexing the corresponding peaks using standard diffraction files of apatite (JCPDS# 09-0432), α -TCP (JCPDS# 09-0348), β -TCP (JCPDS# 09-0169), CaO (JCPDS# 37-1497), $\text{Ca}(\text{OH})_2$ (JCPDS# 04-0733) and CaCO_3 (JCPDS# 29-0305).

2.5.2. FTIR characterization

FTIR transmittance spectra are obtained in the 4000–450 cm^{-1} infrared region. The obtained spectra is compared to the standard KBr and reference materials and compared to correlation charts for more precise assignments of the observed vibrational peaks.

3. Results and discussions

3.1. Crystallinity analyses using X-ray diffractometry

The XRD patterns of the samples displayed in Figure 1 show the characteristic peaks of HAp and TCP. Although there are TCPs present, however, majority of the peaks belong to HAp. The presence of α -TCP affects the degree of crystallinity of the obtained biological HAp powders in view of the fact that TCP competes with HAp formation and causes distortions on the HAp crystal.

However, it is worth noting that as the amount of CaCO_3 is increased, the presence of α -TCP and β -TCP peaks become noticeably reduced with increasing growth of HAp peaks. The reason why the TCP peak weakens might be that TCP undergoes transition to HAp phase upon addition of CaCO_3 . This implies the possibility of tailoring HAp phase by subsequent addition of CaCO_3 .

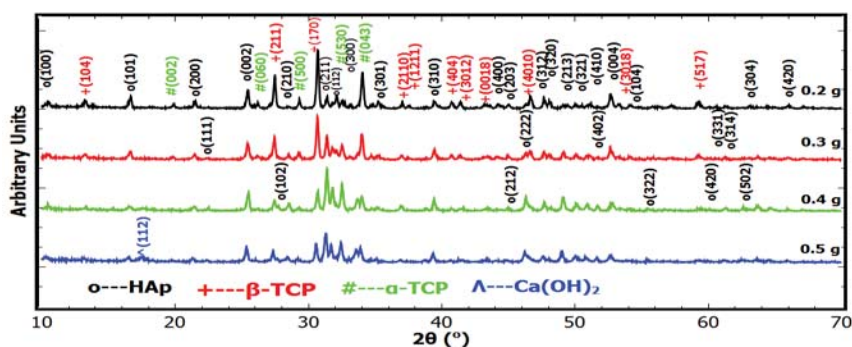


Figure 1. X-ray diffractogram of biological HAp powders with various amounts of CaCO_3 calcined at 900°C .

The HAp powders with [Ca]/[P] ratios 1.42, 1.46, 1.61 and 1.93 have degree of crystallinity equal to 58.08, 72.13, 85.79, 75.85% and crystal size equal to 0.67, 0.74, 0.75, 0.72 nm, respectively. From these results, it can be observed that there is an increasing degree of crystallinity as the amount of CaCO₃ is increased except for the apatite powders with 0.50g CaCO₃ which has degree of crystallinity at 75.85% only. Taking into account the [Ca]/[P] ratio of the obtained HAp powders, it appears that it is the reason why the degree of crystallinity of the biological HAp sample with 0.50 g CaCO₃ decreases. As the [Ca]/[P] ratio approaches the value of 1.67, for stoichiometric HAp, the degree of crystallinity increases as seen from Figure 2a. The HAp sample with [Ca]/[P] ratio closest to 1.67 has the highest degree of crystallinity. However, as [Ca]/[P] ratio goes beyond 1.67, a decrease on the degree of crystallinity is observed. Although the TCP phase is the least in this sample, another impurity which is Ca(OH)₂ is formed which might be from the excess calcium present in the sample.

Considering the crystal size of the HAp samples, the result shows that as the HAp sample becomes stoichiometric, the crystal size increases as seen from Figure 2b. However, crystal size decreases as it goes beyond the stoichiometric ratio. Hence, as the HAp sample becomes crystalline, the crystal size increases. This is due to the increase of the crystallinity which is probably caused by the formation of the crystal structure. The results show that the degree of crystallinity and crystal size are associated with the amount of impurity and the stoichiometry of the obtained biological HAp powders.

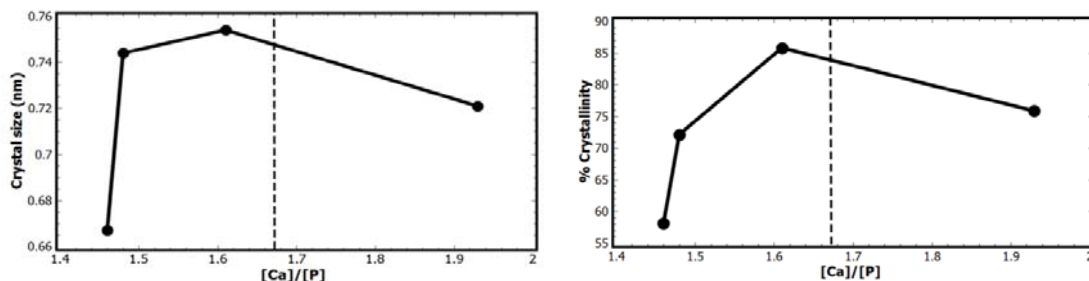


Figure 2. Relationship between (a) Xc and [Ca]/[P] ratio and (b) crystal size with respect to its [Ca]/[P] ratio.

It is worth noting that the degree of crystallinity of the obtained biological HAp samples with [Ca]/[P] ratios 1.42 and 1.48 fall on the range of the desired crystallinity for medical application. Also, the crystal sizes of these samples are at nanolevel and thus have a high surface area for good

resorption. Additionally, resorption can be regulated by combination of several calcium phosphate phases. TCPs are very soluble while HAp is stable. Combination of these two phases makes the obtained biological HAp samples added with CaCO_3 possess the solubility of TCPs and the stability of HAp.

3.2. Crystallinity analyses using FTIR spectroscopy

The powder IR absorption spectra of the investigated samples displayed in Figure 3 show the usual absorption bands of HAp. The intense bands observed at $900\text{--}1200\text{ cm}^{-1}$ and $500\text{--}620\text{ cm}^{-1}$ are related to internal vibrations of the PO_4 tetrahedra. They are referred to as symmetric stretch, bending mode, and anti-symmetric stretch. Another bands related to the stretching of OH groups are observed in the IR spectrum of the HAp samples at 3572 and 3643 cm^{-1} . The OH vibration seen at 3643 cm^{-1} corresponds to $\text{Ca}(\text{OH})_2$. This peak is strongest at the biological HAp sample with 0.5 g CaCO_3 . This may be due to the excess Ca^{2+} ions on the sample that bind with OH^- ion from water or due to the CaO produced from the decomposition of CaCO_3 . Bands related to the adsorbed H_2O are observed at 1634 and 3433 cm^{-1} . Lastly, vibrations corresponding to carbonate group is seen as a singlet peak at 875 cm^{-1} and doublet peak around 1420 and 1461 cm^{-1} . These peaks are contributed from the added CaCO_3 to the biological HAp samples. The spectra of the HAp samples display a systematic splitting of the anti-symmetric stretch and bending mode of PO_4 bands.

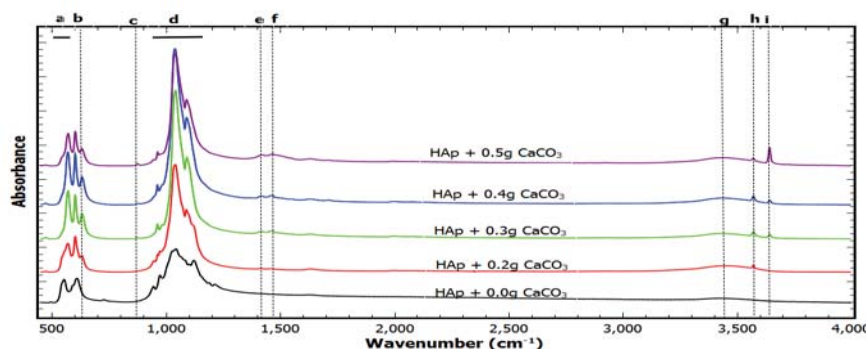


Figure 3. FTIR spectra of biological HAp powders with various amounts of CaCO_3 calcined at 900°C with peaks at (a) 570 and 602 cm^{-1} , (b) 630 cm^{-1} , (c) 875 cm^{-1} , (d) 963 , 1094 and 1089 cm^{-1} , (e) 1420 cm^{-1} , (f) 1461 cm^{-1} (g) 3433 cm^{-1} , (h) 3572 cm^{-1} and (i) 3643 cm^{-1} .

The SF for the apatite samples with $[\text{Ca}]/[\text{P}]$ ratios 1.46 , 1.48 , 1.61 and 1.93 are 14.85 , 16.99 , 19.70 and 15.71 , respectively. The results show that as $[\text{Ca}]/[\text{P}]$ ratio approaches the stoichiometric ratio, the splitting factor increases as seen from Figure 4a. The HAp sample with $[\text{Ca}]/[\text{P}]$ ratio closest to the stoichiometric ratio has the highest splitting factor. However, the splitting factor decreases as the $[\text{Ca}]/[\text{P}]$ ratio exceeds 1.67 . It is worth noting that these results obtain from infrared spectroscopy match the results with % crystallinity obtain from XRD.

At 900 and 1200 cm^{-1} spectral region, a broadening of the spectra is observed between the anti-symmetric stretch modes at 1040 and 1090 cm^{-1} . Incorporation of different types of anions in the HAp unit cell which affects the vibration of PO_4 and induces local structural distortions around these ions might be the reason for the broadening on this region. Thus the area of phosphate-substitution site might give information on the crystal structure of HAp. This research uses the method done by Pleshko [8] on measuring the area of phosphate-substitution site named as band B. The HAp powders added with 0.2 , 0.3 , 0.4 , 0.5 g CaCO_3 has %B equal to 20.88 , 12.42 , 12.03 , 14.85% , respectively. From the results it can be seen from Figure 4b that %B and crystal size has a linear relationship with correlation coefficient (R^2) = 0.994 . This suggests that the decrease of the area of phosphate-substitution site indicates increase in the crystal size. Hence the area of phosphate-substitution site might correspond to the c -axis length of HAp.

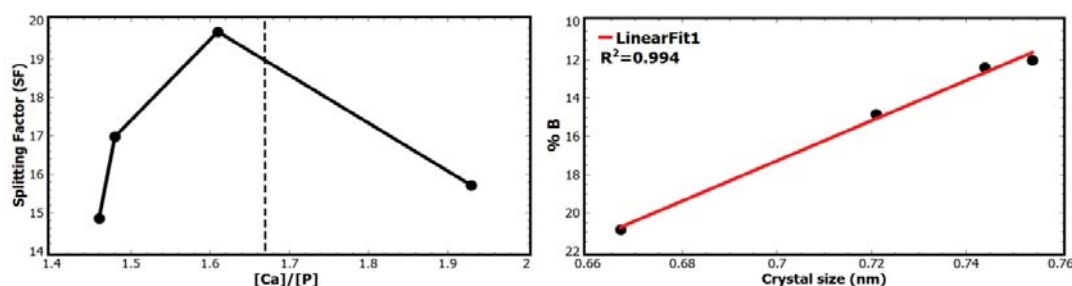


Figure 4. Graph of (a) the splitting factor (taken as the area between peaks 570 and 602 cm^{-1}) as an index of crystallinity with respect to [Ca]/[P] ratio and (b) %B with respect to crystal size showing linear relationship.

4. Conclusions

Engineering of the crystallinity of biological HAp powders from thermally-treated fish bones by addition of CaCO_3 was successfully done. The degree of crystallinity and crystal size of the obtained biological HAp powders were successfully calculated using diffraction planes (300), (112) and (002) in XRD. The indices of crystallinity for biological HAp were established using the splitting factor of the bending mode of PO_4 vibration at 500-620 cm^{-1} and area of phosphate-substitution site of the symmetric-antisymmetric stretching modes of PO_4 vibrations at 900-1200 cm^{-1} in FTIR.

Results show that the degree of crystallinity and crystal size of the obtained biological HAp are influenced by its stoichiometry. By addition of CaCO_3 as source of Ca^{2+} ions, the [Ca]/[P] ratio of the obtained calcium deficient biological HAp powders approaches the stoichiometric ratio. As a result, the degree of crystallinity and crystal size increase. However, crystallinity and crystal size decrease with [Ca]/[P] > 1.67. Hence, engineering the crystallinity and crystal size of the thermally-treated biological HAp can be possible by addition of CaCO_3 . Significantly, degree of crystallinity of the HAp powders with [Ca]/[P] ratio equal to 1.46 and 1.48 fall near the range 60-70% for highly resorbable HAp used for medical application.

The splitting factor of the bending mode of phosphate vibration at 500-620 cm^{-1} matches the result with % crystallinity on XRD. Hence, the splitting factor of phosphate vibration is a good index of crystallinity. Moreover, the area of phosphate-substitution site of PO_4 vibration at 900-1200 cm^{-1} infrared spectral region corresponds to the length of the *c*-axis of HAp. IR spectroscopy and X-ray diffraction are thus both suited to determine crystal size and crystallinity of HAp and should be used in conjunction when possible to obtain the maximum amount of structural information.

References

- [1] Kumar GS, Girijja EK, Thamizhavel A, Yokogawa Y and Kalkura SN 2010 *J. Colloid and Interface Science* **349** 56–62
- [2] Mahabole MP, Aiyer RC, Ramakrishna CV, Sreedhar B and Khairnar RS 2005 *Bull. Mater. Sci.* **28** 535–45
- [3] Mene RU, Mahabole M P and Khairnar R S 2011 *Radiation Physics and Chemistry* **80** 682–7
- [4] Zaragoza DL, Guzman ETR and Gutierrez LRR 2007 *J. Minerals and Materials Characterization and Engineering* **8** 591–609
- [5] Rigano L *et al.* 2009 *SOFW-Journal* **135** 20–7
- [6] Prabakaran K and Rajeswari S 2009 *Spectrochimica Acta Part A* **74** 1127–34
- [7] Fathi MH, Hanifi A and Mortazavi V 2008 *Journal of Materials Processing Technology* **202** 536–42
- [8] Pleshko N, Boskey A and Mendelsohn R 1991 *Biophys. J.* **60** 786–93
- [9] Abraham JA, Sanchez HJ, Marcelli CA, Grenon M, Guidi MC and Piccinini M 2011 *Anal. Bioanal. Chem.* **399** 1699–704
- [10] Landi E, Tampieri A, Celotti Gand Sprio S 2000 *J. Eur. Ceram. Soc.* **20**, 2377–87